The Influence of Near- and Far-field Earthquakes on the Seismic Performance of Base-Isolated Nuclear Power Plant Structures

Van-Binh Tran
Faculty of Engineering and Technology
Ha Tinh University
Ha Tinh, Vietnam
binh.tranvan@htu.edu.vn

Sy-Minh Nguyen
Faculty of Engineering and Technology
Ha Tinh University
Ha Tinh, Vietnam
minh.nguyensy@htu.edu.vn

Tien-Hong Nguyen
Department of Civil Engineering
Vinh University
Vinh, Vietnam
tienhongkxd@vinhuni.edu.vn

Van-Hoa Nguyen
Department of Civil Engineering
Vinh University
Vinh, Vietnam
vanhoakxd@vinhuni.edu.vn

Thi Thuy-Huong Doan
Department of Civil Engineering
Vinh University
Vinh, Vietnam
doanhuongdhv@gmail.com

Duy-Duan Nguyen
Department of Civil Engineering
Vinh University
Vinh, Vietnam
duyduankxd@vinhuni.edu.vn

Abstract-This study aims to investigate the influence of near- and far-field earthquakes on the seismic performance of base-isolated Nuclear Power Plant (NPP) structures. Two earthquake motion groups of near-field and far-field characteristics are selected for fragility evaluation analysis. A base-isolated advanced reactor power 1400 (APR-1400) is employed for numerical analysis. A set of fragility curves are derived for various limit states based on the maximum likelihood estimation. The limit states are defined in terms of Lead Rubber Bearing (LRB) deformation capacity. The numerical results reveal that the median maximum deformations of LRBs were smaller for far-field ground motions than for near-field motions. Also, the comparison of fragility curves demonstrates that the probability of failure of base-isolated NPP structures is higher for near-field ground motions than far-field motions. It is crucial to select earthquake ground motions with both near- and far-field motions for the seismic evaluation of NPP structures.

Keywords-near-field earthquake; far-field earthquake; LRB; fragility analysis; nuclear power plant structure; lumped mass stick model

I. INTRODUCTION

The near-field strong ground motion consists of complex characteristics, mainly affected by the fault rupture velocity, the length of fault rupture, sliding direction, and other factors. Those characteristics can cause significant damage to structures during an earthquake. The influence of near-field earthquakes on the response of civil engineering structures has been numerously investigated in [1-7]. Some of the Nuclear Power Plants (NPPs) in Korea are located near fault ruptures. After the 2016 Gyeongju and 2017 Pohang earthquakes, the seismic safety of NPP structures is getting more and more attention.

Seismic analyses and fragility evaluations of NPP structures were implemented in [8-16]. Among that, remarkably, authors in [9-10] developed the seismic fragility curves of a non-isolated CANDU type NPP containment building for near-field ground motions based on the displacements obtained from the nonlinear time history analyses. Authors in [17] assessed the safety implication of near-field earthquakes on NPP structures designed according to the North American codes. They concluded that the near-field motion effects were not so damaging to the containment which is a relatively stiff structure. However, the effects of near-field forward-directivity, fling-step, and far-field motions on seismic fragility curves of base-isolated NPP structure were not evaluated.

The purpose of this study is to develop seismic fragility curves of a base-isolated APR-1400 NPP structure considering the influence of near- and far-field ground motions. For near-field earthquakes, two typical characteristics, forward-directivity and fling-step are accounted for in fragility analyses. The limit states are defined based on the shear strain capacity of Lead Rubber Bearings (LRBs). A set of fragility curves for limit states are generated using the maximum likelihood estimation. The influence of earthquake groups on fragility curves is also examined.

II. INPUT GROUND MOTIONS

Near-field earthquakes contain a large portion of fault energy in the form of pulses [2]. Pulses can normally be recognized through acceleration, velocity, and displacement time histories. Two typical effects in near-field ground motions are forward-directivity and fling-step phenomena. Forward directivity occurs where the fault rupture propagates with a velocity close to the shear-wave velocity. This is accompanied

by generating long-period, short-duration, and large-amplitude pulses in the velocity time histories. Displacement associated with such a shear-wave velocity is largest in the fault-normal direction for strike-slip faults [1, 3]. On the other hand, fling step effect produces the evolution of residual ground displacement due to the tectonic deformation associated with the rupture mechanism. This is generally characterized by a unidirectional high amplitude velocity pulse and a monotonic step in the displacement time history [2]. Figure 1 illustrates the time-history traces of near- and far-field earthquakes. A high-velocity pulse can be seen in the 1979 Imperial Valley earthquake. For the 1971 San Fernando earthquake, i.e. a far-field motion, no high pulses existed in the time histories. It should be noted that if a motion record has an epicentral distance less than 12km, it is considered as a near-field earthquake, otherwise it is considered a far-field motion [18].

In this study, two different groups of ground motions classified into near-field and ordinary far-field types were considered. For each group, 20 motion records were involved for fragility analysis. All used records were adopted from the PEER center database. Figure 2 shows the response spectra of ground motions in three groups. The thick curve indicates the mean spectrum.
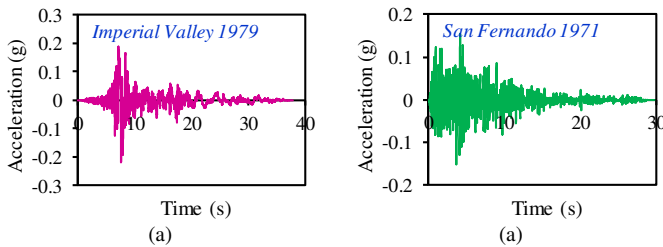

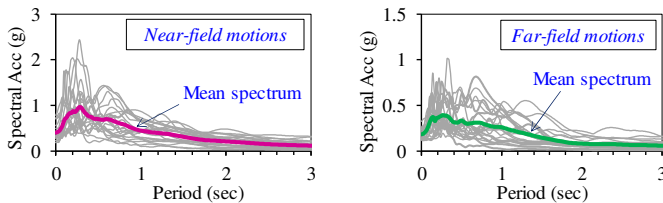Fig. 1.   Example of time-history traces of (a) near- and (b) far-field earthquakes.

Fig. 2.   Spectral accelerations of input ground motions.

III.   STRUCTURAL MODELING

In this study, the advanced power reactor 1400 (APR-1400) developed by Korea Electric Power Corporation, was employed for numerical analysis. We focused our modeling on the Reactor Containment Building (RCB), the Internal Structure (IS), and the Auxiliary Building (AB). The Finite Element Model (FEM) of the base-isolated NPP structure was developed using the Lumped-Mass Stick Model (LMSM) in SAP2000 [19]. The masses and equivalent section properties were calculated based on the designed cross sections of the structures. The structures were modeled in terms of elastic beam elements. Furthermore, elastic shell elements were applied for the base-mat. The lumped masses were assigned to the associated element nodes. Figure 3(a) shows the FEM of

the base-isolated NPP structures and the mechanical properties of LRBs. For the base isolation system, 486 LRBs were installed under the base-mat to enhance the seismic performance of the NPP structures. Figure 3(b) illustrates the bilinear shear force-deformation model of LRBs due to shear forces. The bilinear model of LRB was assumed to be a parallelogram. Therefore, the values of Q_d, F_y, K_u, and K_d in the negative direction are equal to those in the positive. The mechanical properties of LRBs are also described in Figure 3(b). The results of eigenvalue analysis are presented in Figure 4. The result is consistent with the findings in [20-21].

486 LRBs are installed with properties:
- Elastic stiffness, $K_u = 537.703E3$ KN/m
- Post yield stiffness ratio: 0.00782
- Yield strength, $F_y = 1009$ KN
- Characteristic strength, $Q_d = 1001$ kN
- Hardening stiffness, $K_d = 4205$ kN/m
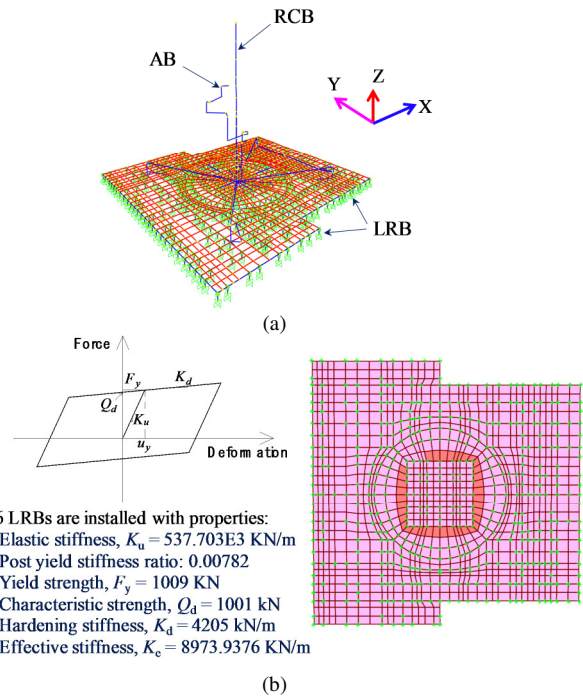- Effective stiffness, $K_e = 8973.9376$ KN/m

(b)

Fig. 3.   FEM of base-isolated NPP structures and bilinear model of LRBs: (a) LMSM of base-isolated NPP structures, (b) arrangement and properties of LRBs.
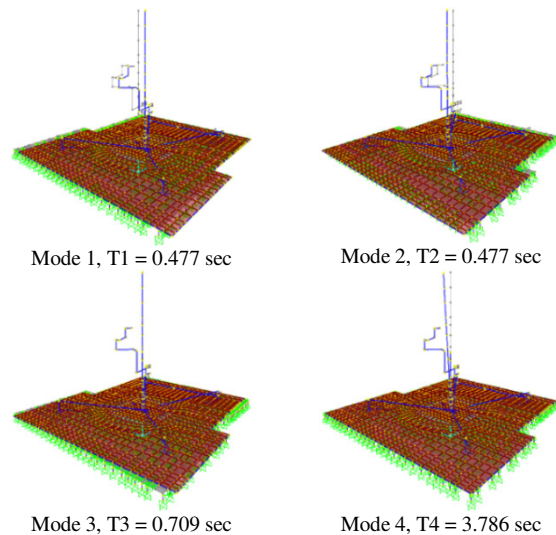

Fig. 4.   Vibration mode shapes of base-isolated NPP structures.

IV. RESPONSE OF NPP STRUCTURES AND FRAGILITY ANANLYSIS

A series of time-history analyses were performed. All ground motions were imposed on the NPP models in the horizontal direction. To evaluate the fragility of the base-isolated NPP structure, the hypothesis that LRB is the critical element was made. The superstructures are expected to vibrate within an elastic range during earthquakes. It is common to quantify the lateral displacement or/and acceleration responses of structures subjected to earthquakes [22-24]. Therefore, the seismic response of the base-isolated model is obtained in terms of the shear deformation behavior of LRBs. Figure 5 shows an example of the behavior of LRB during different types of earthquakes (i.e. near- and far-field motions) with a specified level PGA = 0.4g. It can be found that the deformation responses of LRBs due to near-field earthquakes are significantly larger than that under the far-field motion. Figure 6 shows the maximum lateral deformation of LRBs in various levels of PGA under different earthquake groups. The thick lines represent the mean results. Because of the pulse characteristic, the mean values of deformation of LRBs under near-field earthquakes are higher than those due to ordinary far-field earthquakes.
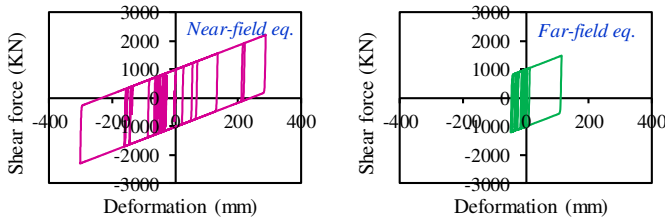

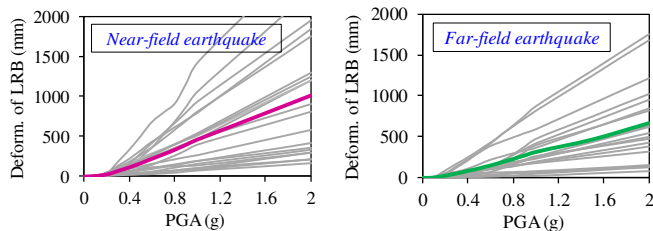Fig. 5.   Hysteretic behavior of LRB under earthquakes with PGA = 0.4g.

Fig. 6.   Incremental displacements of LRB with PGA under near- and far-field earthquakes.

For developing fragility curves, a set of limit states should be pre-defined according to the damage levels of the components. This study used three defined limit states, namely slight, moderate, and extensive. These limit states were determined based on the shear strain of LRB. The shear strain (γ) is expressed by the ratio of the maximum lateral deformation (Δ) and the height of LRB (H). According to recent experimental studies [29-34], the LRB can reach an ultimate capacity of beyond 400% shear strain. We adopted these results to define three limit states, if the shear strain exceeds 100% (i.e. $\Delta \geq 40$cm) the slight limit state (LS1) is specified. If the shear strain goes beyond 200% (i.e. $\Delta \geq 80$cm) and 300% (i.e. $\Delta \geq 120$cm) the moderate (LS2) and extensive (LS3) limit states are respectively established.

Among several methods to develop seismic fragility curves, the Maximum Likelihood Estimation (MLE) approach [25] was used in this study. In this approach, the fragility function is assumed as a log-normal Cumulative Distribution Function (CDF) expressed by:

$$F_k(a) = \Phi\left[\frac{\ln(a/c_k)}{\zeta_k}\right] \quad (1)$$

where a is the earthquake intensity, namely PGA in this study, c_k and ζ_k are the median and the log-standard deviations of the log-normal CDF, and $\Phi(-)$ is the standard normal CDF. In (1), the subscript k indicates the k-th limit state when more than one limit state is considered. In the MLE, c_k and ζ_k are determined by maximizing the likelihood function. This function is defined by:

$$L = \prod_{i=1}^{N}[F_k(a_i)]^{x_i}[1 - F_k(a_i)]^{(1-x_i)} \quad (2)$$

where $F_k(a)$ increases when damage occurs and $1 - F_k(a)$, the probability of not experiencing a damage, increases when damage does not occur for an earthquake intensity a_i. N is the number of ground motions considered and x_i is a Bernoulli random variable that indicates whether the structure is damaged or not where 0 indicates no damage and 1 indicates damage. c_k and ζ_k are determined so that (2) is maximized with respect to c_k and ζ_k as follows:

$$\frac{\partial L}{\partial c_k} = \frac{\partial L}{\partial \zeta_k} = 0, \quad k = 1, \cdots, N_{state} \quad (3)$$

where N_{state} is the number of limit states.

Fragility curves of base-isolated NPP structures were developed for the 3 limit states considering the three groups of ground motions. Figure 7 shows the fragility curves for the 3 limit states with different earthquake groups. It can be observed that the base-isolated NPP structure might behave as without damage if the level of PGA less than 0.6g, which is significantly higher than the operational basis earthquake design level of APR-1400 NPP structures. Additionally, the isolated structure suffered no damage within PGA 0.8g of far-field earthquakes.
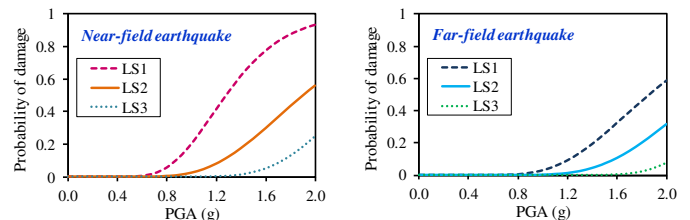

Fig. 7.   Seismic fragility curves of base-isolated NPP structures subjected to near- and far-field earthquakes

Figure 8 shows the comparison of fragility curves for the three groups of earthquakes. It can be observed that the structural model under near-field motions is more vulnerable than that due to far-field earthquakes. This can be attributed to the obvious reason that the deformation of LRBs produced by near-field motions is higher than that under far-field motions.
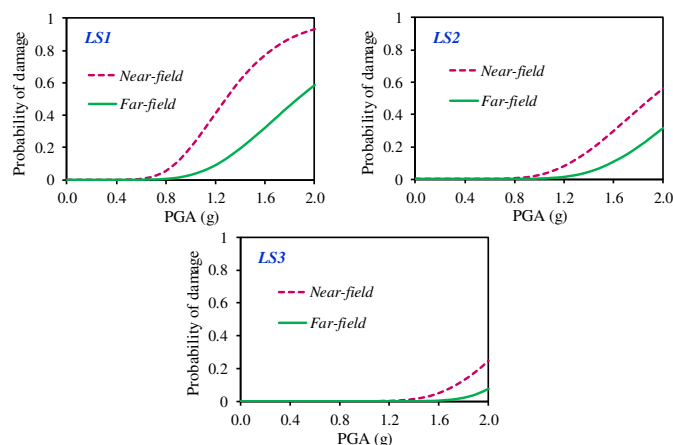
Fig. 8.   Comparison of fragility curves of base-isolated NPP structures in different defined limit states.

V.   CONCLUSIONS

In this study, seismic fragility curves of the base-isolated APR1400 NPP structures were derived for different limit states based on the maximum likelihood estimation. The influence of near-field and far-field ground motions was considered. Based on the numerical results, the following conclusions are drawn.

- The maximum deformations of LRBs were shown to be smaller for far-field earthquakes than for near-field ground motions. This is due to the high-amplitude pulse effect of near-field motions.

- The probability of failure of base-isolated NPP structures is significantly higher for near-field ground motions compared to that for far-field earthquakes.

- The NPP model has not suffered any damage within PGA 0.6g, which is higher than the safe shutdown earthquake design level of APR-1400 NPP structures.

- It is crucial to select earthquake ground motions with both near- and far-field motions for the seismic evaluation of NPP structures.

REFERENCES

[1] E. Kalkan and S. K. Kunnath, "Effects of Fling Step and Forward Directivity on Seismic Response of Buildings," *Earthquake Spectra*, vol. 22, no. 2, pp. 367–390, May 2006, https://doi.org/10.1193/1.2192560.

[2] M. Bhandari, S. D. Bharti, M. K. Shrimali, and T. K. Datta, "The Numerical Study of Base-Isolated Buildings Under Near-Field and Far-Field Earthquakes," *Journal of Earthquake Engineering*, vol. 22, no. 6, pp. 989–1007, Jul. 2018, https://doi.org/10.1080/13632469.2016.1269698.

[3] R. Eskandari and D. Vafaei, "Effects of near-fault records characteristics on seismic performance of eccentrically braced frames," *Structural Engineering and Mechanics*, vol. 56, no. 5, pp. 855–870, 2015, https://doi.org/10.12989/sem.2015.56.5.855.

[4] A. Karbassi, H. Hamidi, and P. Lestuzzi, "Fling-step effect on the seismic behavior of high-rise RC buildings during the Christchurch earthquake," Wellington, New Zealand, Feb. 2013.

[5] M. Zhang, G. Parke, and Z. Chang, "The dynamic response and seismic damage of single-layer reticulated shells subjected to near-fault ground motions," *Earthquakes and Structures*, vol. 14, no. 5, pp. 399–409, 2018, https://doi.org/10.12989/eas.2018.14.5.399.

[6] W.-I. Liao, C.-H. Loh, and B.-H. Lee, "Comparison of dynamic response of isolated and non-isolated continuous girder bridges subjected to near-fault ground motions," *Engineering Structures*, vol. 26, no. 14, pp. 2173–2183, Dec. 2004, https://doi.org/10.1016/j.engstruct.2004.07.016.

[7] S. Zhang and G. Wang, "Effects of near-fault and far-fault ground motions on nonlinear dynamic response and seismic damage of concrete gravity dams," *Soil Dynamics and Earthquake Engineering*, vol. 53, pp. 217–229, Oct. 2013, https://doi.org/10.1016/j.soildyn.2013.07.014.

[8] Y. Pan, C. E. Ventura, and W. D. Liam Finn, "Effects of Ground Motion Duration on the Seismic Performance and Collapse Rate of Light-Frame Wood Houses," *Journal of Structural Engineering*, vol. 144, no. 8, Aug. 2018, Art. no. 04018112, https://doi.org/10.1061/(ASCE)ST.1943-541X.0002104.

[9] S. H. Eem, H. J. Jung, M. K. Kim, and I. K. Choi, "Seismic Fragility Evaluation of Isolated NPP Containment Structure Considering Soil-Structure Interaction Effect," *Journal of the Earthquake Engineering Society of Korea*, vol. 17, no. 2, pp. 53–59, 2013, https://doi.org/10.5000/EESK.2013.17.2.053.

[10] I.-K. Choi, Y.-S. Choun, S.-M. Ahn, and J.-M. Seo, "Seismic fragility analysis of a CANDU type NPP containment building for near-fault ground motions," *KSCE Journal of Civil Engineering*, vol. 10, no. 2, pp. 105–112, Mar. 2006, https://doi.org/10.1007/BF02823928.

[11] I.-K. Choi, Y.-S. Choun, S.-M. Ahn, and J.-M. Seo, "Probabilistic seismic risk analysis of CANDU containment structure for near-fault earthquakes," *Nuclear Engineering and Design*, vol. 238, no. 6, pp. 1382–1391, Jun. 2008, https://doi.org/10.1016/j.nucengdes.2007.11.001.

[12] Q. He, X. Li, Y. Li, A. Liu, and J. Zhang, "Dynamic Nonlinear Time-History Analysis of Nuclear Power Plant under Near-Fault Ground Motion with Velocity Pulse," in *Seventh China-Japan-US Trilateral Symposium on Lifeline Earthquake Engineering*, Aug. 2017, pp. 242–249, https://doi.org/10.1061/9780784480342.033.

[13] E. Lee, J. Kim, K. Joo, and H. Kim, "Evaluation of the Soil-structure Interaction Effect on Seismically Isolated Nuclear Power Plant Structures," *Journal of the Earthquake Engineering Society of Korea*, vol. 20, no. 6, pp. 379–389, 2016, https://doi.org/10.5000/EESK.2016.20.6.379.

[14] G.-J. Kim, K.-K. Yang, B.-S. Kim, H.-J. Kim, S.-J. Yun, and J.-K. Song, "Seismic Response Evaluation of Seismically Isolated Nuclear Power Plant Structure Subjected to Gyeong-Ju Earthquake," *Journal of the Earthquake Engineering Society of Korea*, vol. 20, no. 7_spc, pp. 453–460, 2016, https://doi.org/10.5000/EESK.2016.20.7.453.

[15] J.-H. Lee and J.-K. Song, "Seismic Fragility Analysis of Seismically Isolated Nuclear Power Plant Structures using Equivalent Linear- and Bilinear-Lead Rubber Bearing Model," *Journal of the Earthquake Engineering Society of Korea*, vol. 19, no. 5, pp. 207–217, 2015, https://doi.org/10.5000/EESK.2015.19.5.207.

[16] D. Van Nguyen, D. Kim, and D. Duy Nguyen, "Nonlinear seismic soil-structure interaction analysis of nuclear reactor building considering the effect of earthquake frequency content," *Structures*, vol. 26, pp. 901–914, Aug. 2020, https://doi.org/10.1016/j.istruc.2020.05.013.

[17] K. Galal and A. Ghobarah, "Effect of near-fault earthquakes on North American nuclear design spectra," *Nuclear Engineering and Design*, vol. 236, no. 18, pp. 1928–1936, Sep. 2006, https://doi.org/10.1016/j.nucengdes.2006.02.002.

[18] A. K. Chopra and C. Chintanapakdee, "Comparing response of SDF systems to near-fault and far-fault earthquake motions in the context of spectral regions," *Earthquake Engineering & Structural Dynamics*, vol. 30, no. 12, pp. 1769–1789, 2001, https://doi.org/10.1002/eqe.92.

[19] "SAP2000." Computers and structures Inc, Berkeley, CA, USA, 2013.

[20] D. D. Nguyen and C. N. Nguyen, "Seismic Responses of NPP Structures Considering the Effects of Lead Rubber Bearing," *Engineering, Technology & Applied Science Research*, vol. 10, no. 6, pp. 6500–6503, Dec. 2020, https://doi.org/10.48084/etasr.3926.

[21] D.-D. Nguyen, B. Thusa, and T.-H. Lee, "Effects of Significant Duration of Ground Motions on Seismic Responses of Base-Isolated Nuclear Power Plants," *Journal of the Earthquake Engineering Society of Korea*, vol. 23, no. 3, pp. 149–157, 2019, https://doi.org/10.5000/EESK.2019.23.3.149.

[22] J. A. Alomari, "Effect of the Presence of Basements on the Vibration Period and Other Seismic Responses of R.C. Frames," *Engineering, Technology & Applied Science Research*, vol. 9, no. 5, pp. 4712–4717, Oct. 2019, https://doi.org/10.48084/etasr.3005.

[23] T. Nagao, "An Experimental Study on the Way Bottom Widening of Pier Foundations Affects Seismic Resistance," *Engineering, Technology & Applied Science Research*, vol. 10, no. 3, pp. 5713–5718, Jun. 2020, https://doi.org/10.48084/etasr.3590.

[24] P. C. Nguyen, B. Le-Van, and S. D. T. V. Thanh, "Nonlinear Inelastic Analysis of 2D Steel Frames : An Improvement of the Plastic Hinge Method," *Engineering, Technology & Applied Science Research*, vol. 10, no. 4, pp. 5974–5978, Aug. 2020, https://doi.org/10.48084/etasr.3600.

[25] M. Shinozuka, M. Q. Feng, J. Lee, and T. Naganuma, "Statistical Analysis of Fragility Curves," *Journal of Engineering Mechanics*, vol. 126, no. 12, pp. 1224–1231, Dec. 2000, https://doi.org/10.1061/(ASCE)0733-9399(2000)126:12(1224).